The Astrophysical Journal, 753:158 (11pp), 2012 July 10 doi:10.1088/0004-637X/753/2/158
© 2012. The American Astronomical Society. All rights reserved. Printed in the U.S.A.

HST AND OPTICAL DATA REVEAL WHITE DWARF COOLING, SPIN, AND PERIODICITIES IN GW LIBRAE 3–4 YEARS AFTER OUTBURST[*]

Paula Szkody[1,10,11], Anjum S. Mukadam[1], Boris T. Gänsicke[2], Arne Henden[3], Edward M. Sion[4], Dean Townsley[5], Paul Chote[6,11], Diane Harmer[7], Eric J. Harpe[8], J. J. Hermes[9], Denis J. Sullivan[6,11], and D. E. Winget[9]
[1] Department of Astronomy, University of Washington, Seattle, WA 98195, USA; szkody@astro.washington.edu, mukadam@astro.washington.edu
[2] Department of Physics, University of Warwick, Coventry CV4 7AL, UK; boris.gaensicke@warwick.ac.uk
[3] AAVSO, 49 Bay State Road, Cambridge, MA 02138, USA; arne@aavso.org
[4] Department of Astronomy & Astrophysics, Villanova University, Villanova, PA 19085, USA; edward.sion@villanova.edu
[5] Department of Physics & Astronomy, University of Alabama, Tuscaloosa, AL 35487, USA; Dean.M.Townsley@ua.edu
[6] School of Chemical & Physical Sciences, Victoria University of Wellington, New Zealand; denis.sullivan@vuw.ac.nz, paul.chote@vuw.ac.nz
[7] National Optical Astronomy Observatories, 950 North Cherry Avenue, Tucson, AZ 85726, USA; diharmer@noao.edu
[8] Heritage High School, 7825 NE 130th Avenue, Vancouver, WA 98682, USA; Eric.Harpe@evergreenps.org
[9] Department of Astronomy, University of Texas, Austin, TX 78712, USA; dew@astro.as.utexas.edu
Received 2012 March 15; accepted 2012 May 9; published 2012 June 25

ABSTRACT

Since the large amplitude 2007 outburst which heated its accreting, pulsating white dwarf, the dwarf nova system GW Librae has been cooling to its quiescent temperature. Our *Hubble Space Telescope* ultraviolet spectra combined with ground-based optical coverage during the third and fourth year after outburst show that the fluxes and temperatures are still higher than quiescence ($T = 19{,}700$ K and 17,300 K versus 16,000 K pre-outburst for a $\log g = 8.7$ and $d = 100$ pc). The $K_{\rm wd}$ of 7.6 ± 0.8 km s^{-1} determined from the C I λ1463 absorption line, as well as the gravitational redshift implies a white dwarf mass of $0.79 \pm 0.08\,M_\odot$. The widths of the UV lines imply a white dwarf rotation velocity $v \sin i$ of 40 km s^{-1} and a spin period of 209 s (for an inclination of 11 deg and a white dwarf radius of 7×10^8 cm). Light curves produced from the UV spectra in both years show a prominent multiplet near 290 s, with higher amplitude in the UV compared to the optical, and increased amplitude in 2011 versus 2010. As the presence of this set of periods is intermittent in the optical on weekly timescales, it is unclear how this relates to the non-radial pulsations evident during quiescence.

Key words: binaries: close – binaries: spectroscopic – novae, cataclysmic variables – stars: dwarf novae – stars: individual (GW Lib)

Online-only material: color figures

1. INTRODUCTION

The dwarf nova GW Librae has undergone two very large amplitude outbursts, the first during its discovery in 1983 (Gonzalez & Maza 1983) and the second in 2007 April (Templeton et al. 2007). While it was $V = 17.0$ mag (Thorstensen et al. 2002) during its long quiescence, it reached 8th magnitude at outburst. Its very short orbital period of 76.78 minutes (Thorstensen et al. 2002) and long outburst recurrence time are consistent with very low accretion rate dwarf novae (Howell et al. 1995). This low accretion at quiescence allows a view of the white dwarf, which was found to show non-radial pulsations at 648, 376, and 236 s (Warner & van Zyl 1998; van Zyl et al. 2000, 2004). Ultraviolet observations with the Space Telescope Imaging Spectrograph (STIS) showed the same pulse periods with amplitudes 6–17 times higher than the optical (Szkody et al. 2002), consistent with limb-darkening effects in the atmospheres of stellar pulsators (Robinson et al. 1995). The 2002 UV spectrum revealed a hot white dwarf at ∼15,000 K for $\log g = 8.0$; this temperature places GW Lib near the blue edge of the instability strip for accreting pulsating white dwarfs (Szkody et al. 2010) prior to its outburst. Townsley et al. (2004) used the pulsation periods and the UV data to estimate a high mass of $1.02\,M_\odot$ for the white dwarf.

The 2007 outburst was well studied and provided several interesting avenues for determining various parameters of GW Lib. A superhump present soon after outburst (Kato et al. 2008), used with the orbital period and the empirical relation of Patterson et al. (2005), gave a mass ratio $M_2/M_1 = 0.06$. A narrow emission component from the irradiated donor star provided a K velocity (82 ± 5 km s^{-1}) and systemic velocity (-15 ± 5 km s^{-1}) for the system (van Spaandonk et al. 2010b). As the white dwarfs in dwarf novae are known to be heated by their outbursts (Long et al. 1994; Sion et al. 1998; Piro et al. 2005; Godon et al. 2006), GW Lib presents the unique opportunity to determine the effect of the outburst on the interior of the white dwarf by following the pulsations. The expectation is that the pulsations will stop as the heating causes the white dwarf to move out of the instability strip, and then resume, possibly with shorter periods than previously observed during quiescence, as the white dwarf cools and re-enters the blue edge of the instability strip. A shorter-period post-outburst can arise for two reasons: a higher surface temperature may excite shorter-period modes (Arras et al. 2006) or the higher temperature surface layer can increase the local buoyancy (Townsley et al. 2004). However, a computation of the effect of a heated outer

---

[*] Based on observations made with the NASA/ESA *Hubble Space Telescope*, obtained at the Space Telescope Science Institute, which is operated by the Association of Universities for Research in Astronomy, Inc., (AURA) under NASA contract NAS 5-26555, with the Apache Point Observatory 3.5 m telescope which is owned and operated by the Astrophysical Research Consortium.

[10] Visiting Astronomer, Kitt Peak National Observatory, National Optical Astronomy Observatory, which is operated by the Association of Universities for Research in Astronomy (AURA) under cooperative agreement with the National Science Foundation.

[11] Visiting Astronomer, Mt. John University Observatory, operated by the Department of Physics, University of Canterbury, New Zealand.

layer on the *g*-mode spectrum of a white dwarf, let alone a rapidly rotating one, has not yet been performed. It is possible that the low-order eigenmodes are affected in a non-obvious way. If the white dwarfs are like the H-rich, DA white dwarf pulsators (ZZ Ceti), where the thermal timescale at the base of the convection zone determines which periods will be excited (Montgomery 2005), the periods observed should move from short to longer values as the star cools and the convection zone moves deeper into the star. This scenario is consistent with the observed results for ZZ Ceti pulsators, where those closer to the red edge of the instability strip have longer periods than the hotter pulsators near the blue edge (Clemens 1993; Mukadam et al. 2006). The re-appearance and subsequent evolution of the pulsation spectrum allows an important constraint on the depth of heating that occurs during the outburst. As the mass transfer in accreting, pulsating white dwarfs likely result in different compositions, increased rotation, and increased heating compared to ZZ Ceti stars, their study will help us grasp how these parameters affect the non-radial pulsations.

Follow-up near-UV and optical photometry for the 3 years following the outburst of GW Lib (Copperwheat et al. 2009; Schwieterman et al. 2010; Bullock et al. 2011; Vican et al. 2011) showed decreasing temperatures with a long period near 4 hr and a quasi-period at 19 minutes (evident for 2–4 months) attributed to disk phenomena but no evidence for the return of the non-radial pulsations. The optical magnitude remained at about 0.5 mag above its quiescent level.

We accomplished *Hubble Space Telescope* (*HST*) ultraviolet observations in 2010–2011 to follow the final return of GW Lib to its quiescent temperature. This paper presents our results together with ground-based observations conducted during this same interval.

2. OBSERVATIONS

The observations from space and ground took place during 2010–2011, the third and fourth years after the large amplitude dwarf nova outburst of GW Lib.

2.1. *HST Ultraviolet Spectra*

Two sets of ultraviolet spectra were obtained with the Cosmic Origins Spectrograph (COS). Observations during five *HST* orbits took place on 2010 March 9; the first four with the G160M grating and the last one with G140L. The G160M observations covered a wavelength range of 1405–1775 Å with a resolution of ∼0.07 Å, while the G140L has a wider bandpass (1130–2000 Å) with lower resolution (∼0.75 Å). The wavelength ranges that provided useful data for GW Lib were 1388–1558 and 1579–1748 Å for G160M and 1130–1860 Å for G140L.

The second set of spectra was obtained during two *HST* orbits on 2011 April 9, using the G140L grating for both orbits. The time-tag data were analyzed with PyRAF routines from the STSDAS task package hstcos (version 3.14). The summed spectrum from each grating was extracted with a series of widths to optimize the signal-to-noise ratio (S/N). For the G160M grating with setting 1577, an extraction width of 27 pixels was used as opposed to the default value of 35 for the primary science aperture (PSA). The optimum extraction for the G140L grating setting of 1105 was 41 pixels versus the default value of 57. The four orbits of G160M data were phased on the orbital period of GW Lib and binned into 10 phase bins. These data were used to study the orbital velocity of the white dwarf and its rotation.

Light curves were created from all the spectra by summing the fluxes over all useful wavelengths on several short timescales (3–30 s) to search for variability on orbital and pulsation timescales. Light curves were created after deleting the emission lines from the data in order to reduce the contribution from the accretion disk, and focus on the white dwarf variability. The light curves were divided by the mean and then one was subtracted to place them on a fractional amplitude scale which was used for Discrete Fourier Transform (DFT) analysis. A log of the *HST* observations is given in Table 1.

2.2. *Ground-based Optical Photometry*

Optical photometry was planned close to the times of *HST* observation, both to ensure that GW Lib was close to its quiescent brightness (required by *HST*) and to monitor the return of pulsations. AAVSO observations provided brightness measurements before, during, and following the *HST* times and are available through their archive.[12] These data showed that GW Lib was at a *V* magnitude near 16.5 in 2010 and 16.75 in 2011. Four nights of time-series photometry on larger telescopes with broadband blue filters were obtained in the 2010 season and 16 nights during 2011. Six different telescopes were used during these times with broadband blue bandpass filters. The 2.1 m and 0.9 m telescopes at McDonald Observatory (MO) were used with BG40 filters; the 2.1 m with the Argos time-series CCD (Nather & Mukadam 2004), and the 0.9 m with a comparable CCD called Raptor. The 3.5 m at Apache Point Observatory (APO) also employed the same filter and a similar frame-transfer CCD which is called Agile (Mukadam et al. 2011a) and the Mt. John University Observatory (MJUO) 1 m telescope in New Zealand used the same CCD camera and filter as in Agile and is called Puoko-Nui. The Las Cumbres Observatory Global Telescope network 2 m Faulkes Telescope South (FTS) provided observations with a Fairchild CCD and Bessell B filter. The Kitt Peak National Observatory (KPNO) 2.1 m telescope with the STA2 CCD and BG39 filter was used for short runs on several nights. A summary of these observations is also given in Table 1. The optical data were converted to fractional amplitude in the same way as the *HST* data and used to compute DFTs.

2.3. *Optical Spectra*

One optical spectrum was obtained on 2010 May 5 with the Dual Imaging Spectrograph (DIS), using the high-resolution grating (2 Å) and a 1.5 arcsec slit. One 600 s exposure produced a blue spectrum from 4000–5150 Å and a red spectrum from 6275–7375 Å.

3. RESULTS

Due to the larger wavelength coverage, the lower resolution G140L spectra were used for temperature determination through fits to white dwarf models and a subsequent cooling curve. The higher resolution G160M spectra were used for line measurements to construct a radial velocity curve for the white dwarf and line width fitting to determine the rotation of the white dwarf. All spectra were used to search for pulsations through the creation of light curves. These results are described in detail below.

3.1. *Cooling Curve*

We have three available UV spectra of GW Lib with which to determine the white dwarf temperature: the four orbits at

---

[12] http://www.aavso.org/data-access

Table 1
Summary of Observations

UT Date	Obs.	Tel. (m)	Instr.	Filter	Time	Exp. (s)
2010 Mar 10	MO	0.9	Raptor	BG40	08:25–10:28	30
2010 Mar 11	*HST*	2.4	COS,G160M	. . .	04:09–09:31	Time-tag
2010 Mar 11	*HST*	2.3	COS,G140L	. . .	10:17–11:07	Time-tag
2010 Mar 11	MO	0.9	Raptor	BG40	08:20–12:25	30
2010 Mar 12	MO	2.1	Argos	BG40	10:10–12:23	5
2010 Mar 14	LCOGT	2.0	Fairchild	B	16:57–18:53	25
2010 Mar 15	LCOGT	2.0	Fairchild	B	14:02–18:50	25
2010 May 5	APO	3.5	DIS	. . .	06:47–06:57	600
2011 Mar 2	MJUO	1.0	Puoko-Nui	BG40	13:10–17:23	20
2011 Mar 4	MJUO	1.0	Puoko-Nui	BG40	14:34–16:19	20
2011 Apr 4	APO	3.5	Agile	BG40	10:35–12:05	15
2011 Apr 8	APO	3.5	Agile	BG40	07:26–12:04	15
2011 Apr 9	*HST*	2.4	COS,G140L	. . .	14:08–16:33	Time-tag
2011 May 12	KPNO	2.1	STA2	BG39	06:40–08:44	30
2011 May 13	KPNO	2.1	STA2	BG39	06:23–08:24	30
2011 May 24	KPNO	2.1	STA2	BG39	05:51–08:07	30
2011 May 25	KPNO	2.1	STA2	BG39	05:39–07:46	30
2011 May 26	KPNO	2.1	STA2	BG39	05:50–07:41	30
2011 Jun 9	KPNO	2.1	STA2	BG39	04:58–06:36	30
2011 Jul 1	MJUO	1.0	Puoko-Nui	BG40	07:03–12:07	20
2011 Jul 2	MJUO	1.0	Puoko-Nui	BG40	06:24–11:00	20
2011 Jul 4	MJUO	1.0	Puoko-Nui	BG40	06:36–14:02	20
2011 Jul 6	MJUO	1.0	Puoko-Nui	BG40	06:35–09:28	20
2011 Jul 27	MJUO	1.0	Puoko-Nui	BG40	06:49–12:47	20
2011 Aug 1	MJUO	1.0	Puoko-Nui	BG40	06:40–12:53	20
2011 Aug 2	MJUO	1.0	Puoko-Nui	BG40	06:35–10:04	20

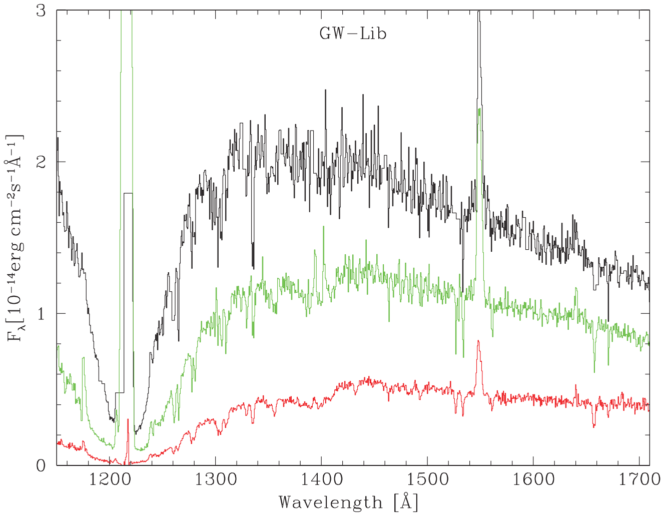

Figure 1. Comparison of STIS spectrum at quiescence (bottom) with COS spectra three years (top) and four years (middle) past outburst.

(A color version of this figure is available in the online journal.)

quiescence with STIS (resolution of 1.2 Å; Szkody et al. 2002) from 2002 January 17, the one orbit of COS G140L at three years past outburst on 2010 March 11, and the two orbits with COS G140L on 2011 April 9 at four years past outburst. Figure 1 shows these three spectra on the same scale, with the COS data binned to the slightly lower resolution of the STIS data. The increased temperature and flux from the post-outburst data are immediately apparent, as is the fact that even at four years past outburst, the white dwarf remains ∼1000 K hotter than its quiescent level.

Table 2
Summary of Best-fit White Dwarf Temperatures

UT Date	Spectrum	Days Past Outburst	Temperature
2002 Jan 17	STIS	Pre-outburst	16,000 K
2008 Apr 17	Optical	371	25,000 K
2010 Mar 11	COS	1064	19,700 K
2011 Apr 9	COS	1458	17,300 K

Since distance and gravity and metal abundance affect the fitting result, we treated all three spectra by using the distance of 100 pc determined from parallax by Thorstensen (2003), adopting a $\log g = 8.7$, corresponding to a mass near $1\,M_\odot$ and using a metal abundance of 0.1 times the solar values. The procedure to determine the white dwarf temperature was similar to that described in Gänsicke et al. (2005). The contribution of the disk was estimated as a blackbody component that accounts for the residual flux in the core of Lyα. In all cases, this component contributes only a few percent, and past experience has shown it does not matter to the temperature fit if a blackbody or power law is used over the short wavelength range. The geocoronal Lyα emission is removed from the fit and the C iv, S iv, and He ii emission lines are treated with broad Gaussians. Then the spectrum is matched with a grid of white dwarf models (Hubeny & Lanz 1995) to find the best fit. The resulting fits are listed in Table 2 and shown in Figure 2. For our fixed $\log g$, the uncertainties in the temperature fits are about 200 K. Decreasing $\log g$ by 0.5 dex decreases the best-fit temperatures by ∼1000 K and increases the distance as these parameters are tied together. The metal abundance will also have a small effect.

To determine a temperature estimate closer to the outburst time, we used the fit (25,000 K) to an optical spectrum obtained on 2008 April 17 (one year after outburst) shown in Bullock et al.

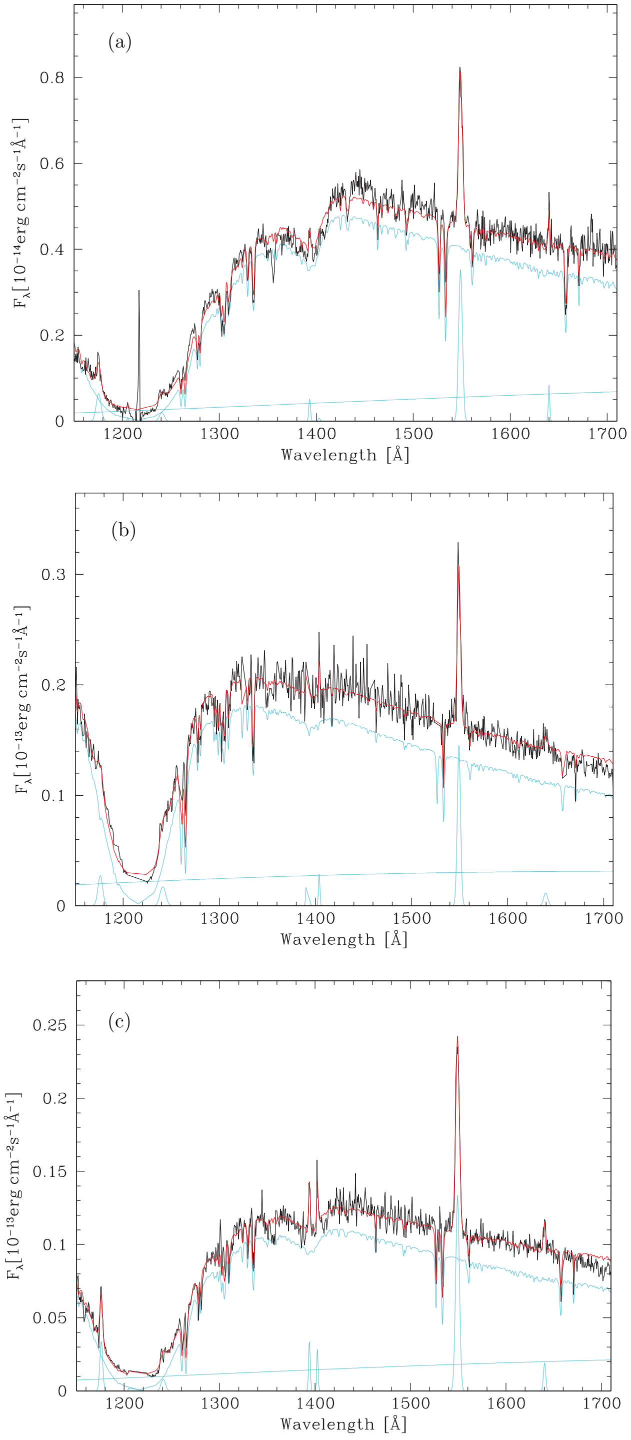

Figure 2. (a) STIS spectrum at quiescence fit with a $T = 16{,}000$ K $\log g = 8.7$ white dwarf model, an accretion disk (lower line), and Gaussians at the emission lines. (b) 2010 COS spectrum three years past outburst fit with a $T = 19{,}700$ K white dwarf model. (c) 2011 COS spectrum four years past outburst fit with a $T = 17{,}300$ K white dwarf model.

(A color version of this figure is available in the online journal.)

Table 3
Radial Velocity Fits

Line	γ (km s^{-1})	K (km s^{-1})	σ (km s^{-1})
C I 1463	29.3 ± 0.1	7.6 ± 0.8	1.7
Si II 1533	34.5 ± 0.1	4.8 ± 1.4	2.9
Al 1670	3.1 ± 0.2	5.4 ± 1.8	3.5
C IV 1550	-95.2 ± 0.1	63.2 ± 7.4	14.7

(2011). However, since the optical is much more contaminated by the disk, this value is not as well determined as the UV temperatures. Figure 3 shows the flux decrease in the blue and red optical spectra obtained at APO on 2010 May 5 in comparison to the 2008 blue optical spectrum. Since the APO spectra were obtained at high airmass compared to the 2008 spectrum (from CTIO), some of the blue decrease may be the result of extinction or refraction. Thus, we only used the 2008 optical and the UV data from 2010 and 2011 for a cooling curve. The resulting temperatures from the available data are shown in Figure 4 along with a one-dimensional quasi-static evolutionary simulation (Sion 1995; Godon et al. 2006) of the heating and subsequent cooling of GW Lib's white dwarf in response to the 2007 outburst. In this simulation, accretion at a high rate was switched on for 23 days to simulate the mass deposition and heating of the outburst. The simulation was carried out for a 1 $M_\odot$ white dwarf. The best agreement with the empirical temperature decline was obtained for an outburst accretion rate of 5×10^{-8} $M_\odot$ yr^{-1}. The curve for GW Lib is very similar in shape to that found for WZ Sge (Godon et al. 2006) but the cooling rate of GW Lib's white dwarf appears to be slower than the WZ Sge degenerate despite having a comparable mass (0.85 $M_\odot$; Steeghs et al. 2007). WZ Sge accreted at a high (outburst) rate for 52 days while GW Lib accreted at its outburst rate for 23 days. However, WZ Sge has a cooler quiescent white dwarf (13,500 K versus 16,000 K) and its outburst amplitude was only 7 mag while GW Lib was 9 mag. Differences in outburst accreted mass, viewing angle, as well as long-term accretion rates may account for the different temperatures in the two systems.

3.2. *Radial Velocity Curves*

The time-tag spectra from the four orbits of optimized high-resolution G160M data obtained in 2010 were binned into 10 phases using the orbital period and taking the start of the observations as the arbitrary zero phase. Absorption lines of C I λ1463, Si II λ 1526,1533, and Al λ1670 were deemed strong enough for useful velocity determination throughout the orbit. These lines were measured singly with IRAF[13] routines "e" which determines a centroid and "k" which uses a Gaussian fit. Since the Si II 1526 line is blended with an interstellar medium component, a procedure that fit the photospheric lines and interstellar component with three Gaussians and only allowed the photospheric lines to move together was tried. This latter procedure showed a mean statistical error on the velocities of 3.6 km s^{-1} but no apparent overall radial velocity variation. However, Gaussian fits from IRAF on the C I line alone produced a noticeable velocity curve. Figure 5 shows the measurements from the single fits to the three lines (Si II is only the 1533 Å component) along with the best-fit sine curve to the velocities to determine γ (systemic velocity) and K (semi-amplitude) using the fixed known period of GW Lib. The solutions are listed in Table 3 along with the total σ of the fit. While only the C I solution ($K = 7.6 \pm 0.08$ km s^{-1}) appears viable, the fits to the other two lines have similar shapes as a function of phase. It is apparent that $K_{\rm wd}$ is very small, much smaller than the past estimates from optical emission lines (38 ± 3 km s^{-1}

---

[13] IRAF (Image Reduction and Analysis Facility) is distributed by the National Optical Astronomy Observatories, which are operated by AURA, Inc., under cooperative agreement with the National Science Foundation.

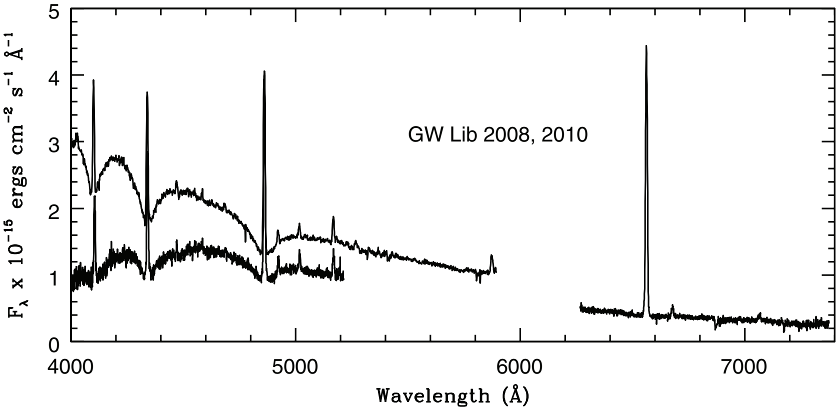

Figure 3. Blue optical spectra of GW Lib obtained in 2008 (top left) and 2010 blue and red spectra (bottom 2 segments).

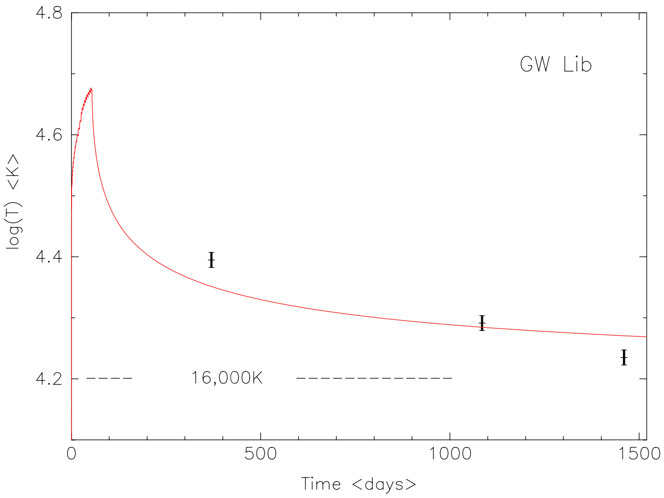

Figure 4. Cooling curve computed for an accretion rate of 5 × 10^{-8} $M_\odot$ yr^{-1} compared to the optical (2008) and UV (2010, 2011) temperature determinations at one to four years post-outburst.

(A color version of this figure is available in the online journal.)

from Thorstensen et al. 2002 and 19.2 ± 5.3 km s^{-1} from van Spaandonk et al. 2010b). Using a narrow Ca II line on the secondary that appeared near outburst to determine $K_{\rm sec}$ in combination with a superhump period excess to determine the mass ratio q, van Spaandonk et al. (2010a) determined $K_{\rm wd}$ of 6.25 ± 0.4 km s^{-1}. This value is consistent with the direct measurement from the C I line. It is also consistent with the center of symmetry of the disk (6 ± 5 km s^{-1}) determined from the Doppler map of the broad Ca II emission (van Spaandonk et al. 2010a). Using $K_{\rm wd}$ from the C I line and $K_{\rm sec}$ from van Spaandonk et al. (2010a) implies a white dwarf mass of 0.79 ± 0.08 $M_\odot$. This value is consistent with the average mass for the white dwarfs in cataclysmic variables, and higher than the masses of single white dwarfs and those in pre-cataclysmic binaries (Zorotovic et al. 2011).

The sine fit to the velocity curve of the C I line can also be used to determine the gravitational redshift of the white dwarf and another estimate for its mass. van Spaandonk et al. (2010a) give an extensive discussion of corrections for systemic velocity as derived from the donor star and Ca II from the disk; we use their value of −18.1 ± 2.0 together with our velocity of 29.3 ± 0.1 for C I (Table 3) to determine $v_{\rm grav}$ (WD) = 47 ± 2 km s^{-1}. This value is similar to that found by van Spaandonk et al. (2010a) from the weak Mg II triplet and consistent with the mass from the K velocity above.

The broad C IV λ1550 emission line was also measured and shows a prominent variation that is offset from the absorption lines. Figure 6 shows the measurements and the sine fit that are listed in Table 3. While the phase shifts of the C, Si, and Al lines are all the same (even though the solutions are poor for Si and Al), the C IV emission is offset by 0.3 phase. van Spaandonk et al. (2010b) pointed out a phase offset of 0.7 phase between the Ca II narrow emission from the secondary and the Ca II broad emission from the accretion disk. Since we do not know the absolute phasing, it is not clear if these offsets are related but it appears that the C IV emission cannot be located in a symmetrical region close to the white dwarf.

3.3. *White Dwarf Rotation*

The high-resolution G160M data also allow an estimate of the rotation of the white dwarf, using the widths of the absorption lines. The white dwarf models were broadened with several rotation rates and compared to the spectrum (Figure 7). The plot shows various rotation rates (20, 50, and 87 km s^{-1} in red, green, and magenta, respectively) for the region of the Si II lines, using a white dwarf model with $T = 17{,}500$ K, log $g = 9.0$ and 0.1 solar abundances. While the $v \sin i$ changes slightly with metal abundance and temperature (Gänsicke et al. 2005), it is clear that the best fit is somewhere near 40 km s^{-1}. For an inclination of 11 deg (van Spaandonk et al. 2010a), the rotation velocity = 210 km s^{-1} and with a white dwarf radius of 7 × 10^8 cm, the rotation period is 209 s. van Spaandonk et al. (2010a) found $v \sin i$ to be 87 ± 3 km s^{-1} using a weak triplet Mg II absorption line in the optical (yielding a rotation period of 97 s for the same parameters of inclination and radius). The deeper, unblended lines apparent in the UV combined with the higher S/N provide a more reliable value for this parameter. The rotation of GW Lib is within the range determined for a few other dwarf novae (for a similar radius, the observed $v \sin i$ implies a period of 63 s for VW Hyi, 110–114 s for WZ Sge, and 400–800 s for U Gem; Sion et al. 1995; Long et al. 2003; Sion et al. 1994). Our result confirms the fast rotation of GW lib compared to single white dwarfs and rules out the spin as the cause of the fine structure with μHz spacing apparent in its pulsation spectrum at quiescence (van Zyl et al. 2004). This fine structure is also apparent in another accreting pulsator SDSS1610-0102 (Mukadam et al. 2010), which has no adequate resolution UV spectrum to confirm its rotation. Note that the spin period of GW Lib does not show up in the quiescent power

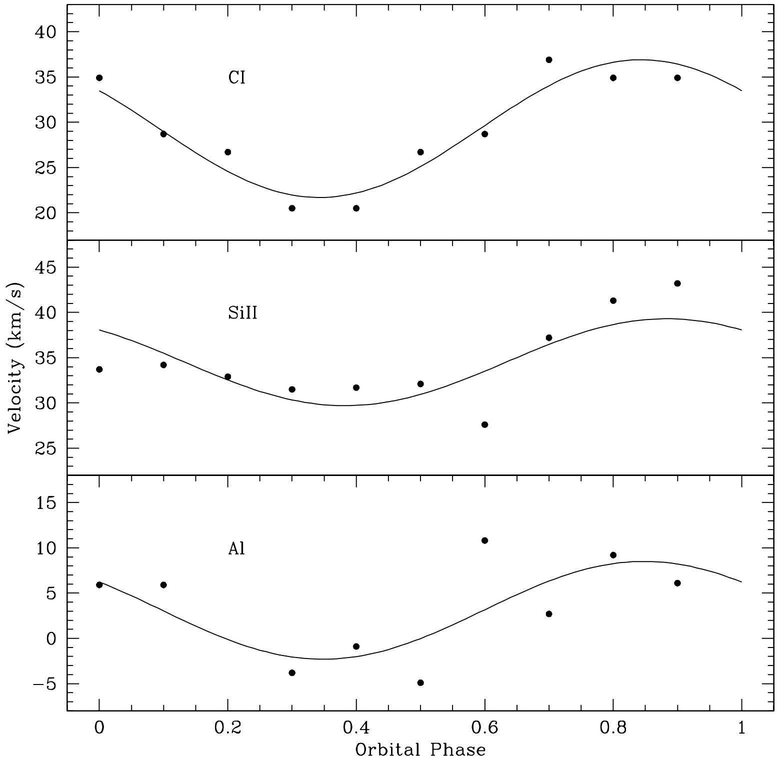

Figure 5. Radial velocities and best-fit sine curves for the C I, Si II, and Al absorption lines from the 2010 G160M binned spectra. Statistical error bars on the fits are 2, 3, and 4 km s^{-1} for C I, Si II, and Al (Table 3). Only C I is significant but others are plotted to show the similar shapes of the fits.

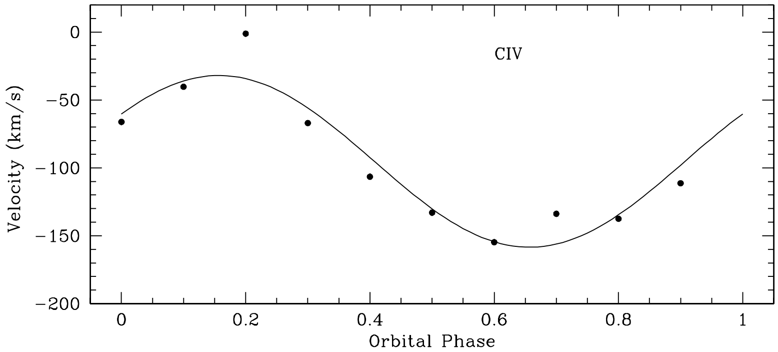

Figure 6. Radial velocities and best-fit sine curve for the C IV emission line from the 2010 G160M binned spectra. Statistical error of the fit is 15 km s^{-1}.

spectrum, as it does in the pulsator V455 And (Araujo-Betancor et al. 2005), so the spectral line fits provide the only means to determine the rotation.

3.4. Light Curves

The UV and optical light curves throughout 2010 and 2011 were treated in a similar manner as in Mukadam et al. (2010). The DFTs were computed for each light curve and the amount of white noise in the light curve was determined empirically by using a shuffling technique (see Kepler 1993). All the best-fit frequencies were initially subtracted to obtain a pre-whitened light curve. Preserving the time column of this light curve, the corresponding intensities were shuffled to destroy any coherent signal while keeping the time sampling intact. A DFT of the shuffled light curve was then computed and its average amplitude was taken as the 1σ limit of white noise. After shuffling the light curve 10 times, the corresponding values for white noise were averaged to determine a reliable 3σ limit. Table 4 lists the 3σ limits for all nights and the periods above this value which were present on at least three nights. The UV data have the advantage of larger amplitudes of pulsation due to limb-darkening effects (Robinson et al. 1995; Szkody et al. 2002). However, the *HST* data are constrained to at most five consecutive orbits with large time gaps between orbits. The optical runs could be longer and gap-free but the southern declination of GW Lib enabled long runs only from the southern hemisphere observatory Mt. John. The 2010 March 14 data had only 36 useful images so no DFT was computed. A long period near 2500 s (41.7 minutes) appears in a good number of data sets, as well as a period near 5100 s (85 minutes). These periods do not appear to be related to the orbital period or even the superhump period seen after outburst. They could be caused by some structure in the disk which has not yet returned to its quiescent state.

The first significant evidence of a short period that could be related to the return of pulsations comes from the COS data of 2010. All five orbits (four of G160M and one of G140L) extracted with 3 s exposures are shown in Figure 8. The fractional intensity variation of each orbit is shown at the

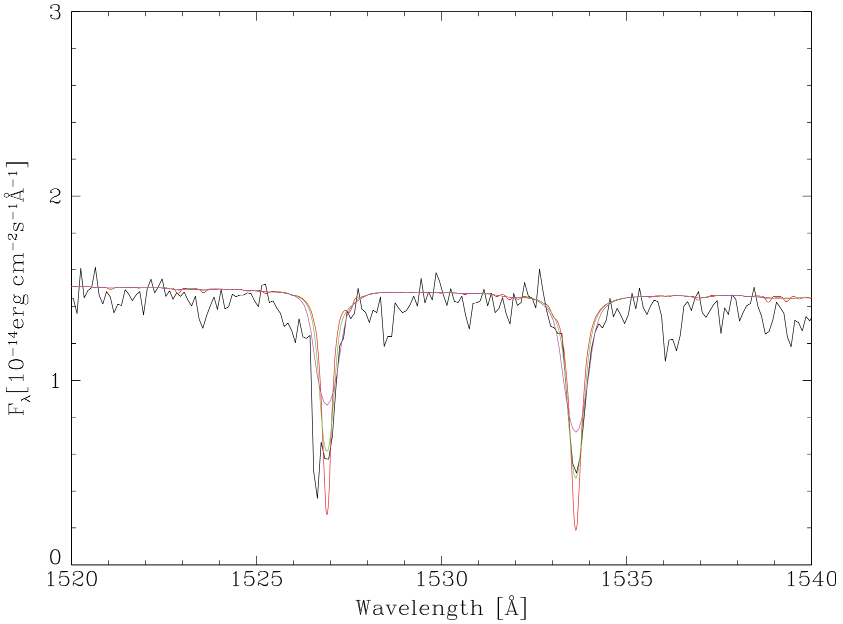

Figure 7. G160M spectra fit with 1 $M_\odot$ white dwarfs with lines broadened by 20 (red), 50 (green), and 87 (magenta) km s^{-1}.
(A color version of this figure is available in the online journal.)

Table 4
Summary of Periodicities

UT Date	Data	Long P (s)	Amp (mma)	Short P (s)	Amp (mma)	3σ
2010 Mar 10	MO	...	...	...	...	9.8
2010 Mar 11	*HST*	...	...	292.0,289.0,282.1,266.0 ± 0.1	19.5,13.5,18.9,7.7 ± 0.7	4.4
2010 Mar 11	MO	2443 ± 33	13.1 ± 1.9	283.6 ± 0.6	9.25 ± 1.9	7.9
2010 Mar 12	MO	...	...	...	...	3.6
2010 Mar 15	FTS	...	...	...	...	8.7
2011 Mar 2	MJUO	2477 ± 44	16.0 ± 2.3	...	...	8.9
2011 Mar 4	MJUO	2525 ± 55	26.8 ± 2.6	...	...	10.4
2011 Apr 4	APO	...	...	276.8 ± 1.7	10.6 ± 2.1	8.8
2011 Apr 8	APO	5132,2563 ± 51,12	14.5,16.6 ± 0.9	275.5,298.5 ± 0.2,0.5	9.7,5.7 ± 0.9	3.8
2011 Apr 9	*HST*	2457 ± 31	14.1 ± 1.4	293.3 ± 0.1	47.2 ± 1.4	5.9
2011 May 12	KPNO	...	...	290,295 ± 5	15,13 ± 18	7.2–12.6[a]
2011 May 13	KPNO	...	...	...	...	9.5
2011 May 24	KPNO	...	...	...	...	10.6
2011 May 25	KPNO	...	...	329.4,313.6 ± 2.1,1.4	9.7,7.5 ± 1.8	7.1
2011 May 26	KPNO	...	...	313.75 ± 0.87	16.2 ± 1.7	7.0
2011 Jun 9	KPNO	...	...	290.8 ± 2.5	8.2 ± 2.4	9.9
2011 Jul 1	MJUO	...	...	281.0 ± 0.2	13.0 ± 1.0	4.0
2011 Jul 2	MJUO	...	...	308.5,300.5,292.5 ± 0.4,0.4,0.2	7.8,13.2,6.5 ± 0.9	3.6
2011 Jul 4	MJUO	5124 ± 32	15.2 ± 0.8	295.0 ± 0.2	9.5 ± 0.8	3.3
2011 Jul 6	MJUO	2592 ± 38	11.5 ± 1.2	286.6 ± 0.3	16.5 ± 1.2	5.0
2011 Jul 27	MJUO	5149,2542 ± 74,13	11.1,14.5 ± 1.1	275.6 ± 0.4	5.5 ± 1.0	4.5
2011 Aug 1	MJUO	2467 ± 27	15.0 ± 3.2	...	...	4.0
2011 Aug 2	MJUO	...	...	323.0 ± 1.0	4.1 ± 0.9	3.8

Notes. [a] Due to the shortness of the light curve, the low frequencies are unresolved so the shuffling technique gives a larger value than normal. A lower limit was found by averaging the white noise from 0.004 to 0.009 Hz.

top, with a view of the entire DFT in the middle and an expanded view of the section around the prominent peak at 0.0035 Hz in the bottom plot. There are four closely spaced periods at 266, 282, 289, and 292 s, with the 292 s period having the highest amplitude (Table 4). The optical data from the McDonald 0.9 m telescope that is simultaneous with part of this time (Table 1) show a period (284 s) within this frequency range (Figure 9). The shorter run on the 2.1 m telescope the next day (with a stricter 3σ) limit does not show any significant feature. The 290 s period appears to be formed of multiple components but the short stretches of data may not be resolving it properly. The 266 s period may be a separate mode.

The two COS orbits in 2011 reveal a periodicity in this same vicinity at 293 s (Figure 10), with an amplitude more than twice as large as the 2010 data. The shorter time span (two orbits in 2011 versus the four in 2010) does not permit the resolution to determine if this feature is also split as in 2010, but the peak is unmistakable. Figure 11 shows a comparison of the G140L data from both years on the top and a comparison of the DFTs on the bottom. The closest optical data sets to the *HST* also

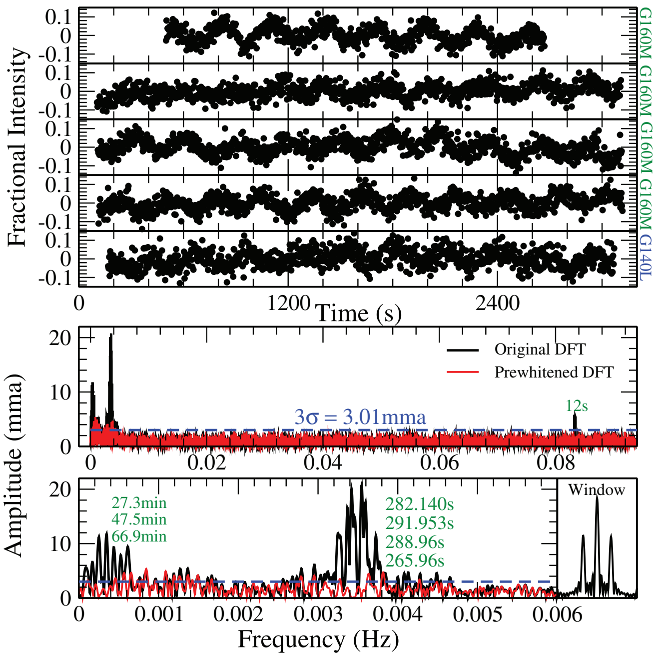

Figure 8. Intensity light curves of all five orbits of *HST* 2010 March 11 data with DFT (middle and expanded at bottom).

(A color version of this figure is available in the online journal.)

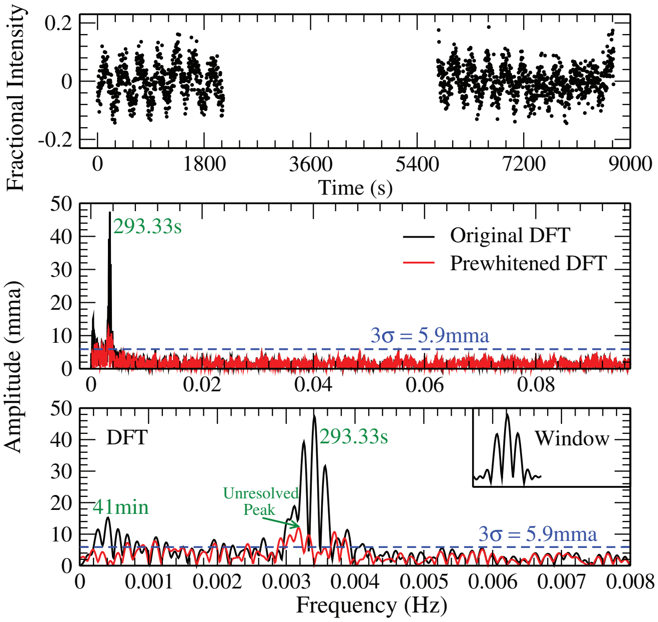

Figure 10. Intensity light curve and DFT for two orbits of *HST* data 2011 April 9.

(A color version of this figure is available in the online journal.)

show significant power near this frequency (Table 4). Figure 12 shows the DFTs for 2011 March–April from the MJUO and APO telescopes.

Further optical data (shorter runs from KPNO in 2011 May–June) and longer runs from Mt. John in 2011 July–August show an intermittent large amplitude periodicity near 290 s is present on some nights (Figures 13 and 14 and Table 4), but absent on others. In addition, as both the *HST* and optical data show, the period is not at exactly the same frequency when it is evident. Other intermittent periods between 300 and 320 s are also apparent. The presence of different periods at different times in ZZ Ceti stars is a known phenomena of amplitude modulation which is not well understood (Kleinman et al. 1998). The appearance of different pulsation frequencies was visible in

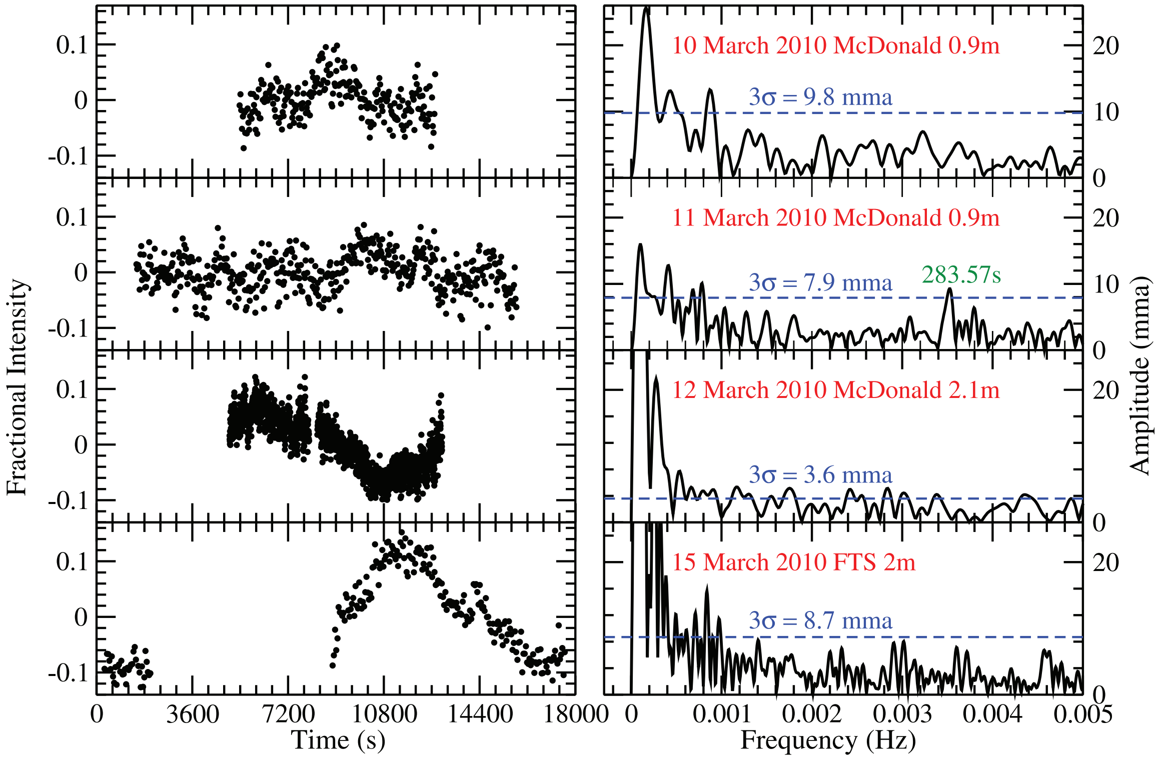

Figure 9. Intensity light curves and DFTs for MO and FTS optical data during 2010 March.

(A color version of this figure is available in the online journal.)

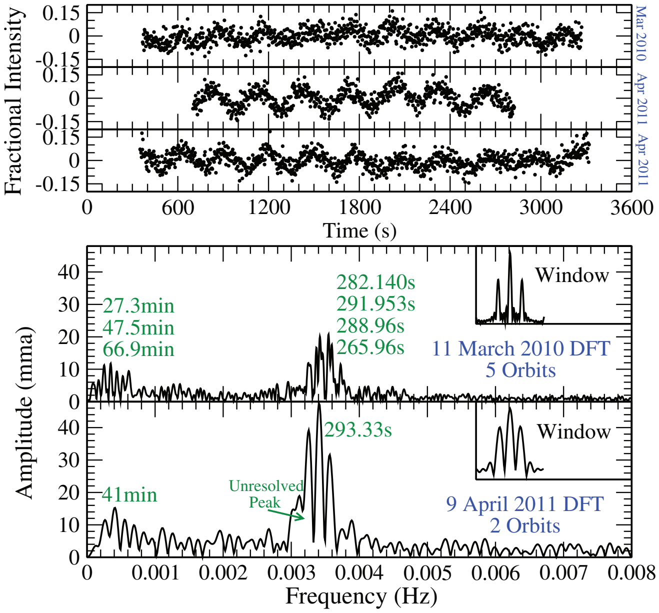

Figure 11. Comparison of 2010 and 2011 G140L light curves (top) and DFTs (bottom where the 2010 DFT is computed from five orbits from G160M and G140L and the 2011 data from two orbits with G140L).

(A color version of this figure is available in the online journal.)

GW Lib at quiescence (van Zyl et al. 2004) and has been seen in the newly discovered accreting pulsators SDSSJ1457+51 and BW Scl at quiescence (Uthas et al. 2012). On the other hand, the pulsations in SDSS0745+45 were observed to occur at the identical frequencies three years after outburst as at quiescence (Mukadam et al. 2011b). Since the pulsation spectrum of GW Lib three to four years after outburst (closely spaced periods near 290 s) compared to quiescence (three periods at 237, 376, and 646 s) is very different, it is difficult to determine whether or not this is the actual return of pulsation. Figure 15 shows a comparison of the light curves and periods from the STIS quiescent data to the COS post-outburst data. Generally, the hotter ZZ Cet stars show the shortest pulsation periods, so shorter periods than quiescence are expected.

4. CONCLUSIONS

Ultraviolet and optical monitoring of GW Lib throughout the three to four years following its large amplitude outburst has revealed the following information.

1. The temperature of the white dwarf continued to decline from 19,700 K at three years to 17,300 K at four years past outburst, but remained above its quiescent temperature of 16,000 K (for a 1 $M_\odot$ white dwarf). During this time, the optical magnitude remained 0.3–0.5 mag above quiescence as well.
2. The best-fit evolution simulation for the available temperatures implies an outburst accretion rate of $5 \times 10^{-8}\ M_\odot\ \mathrm{yr}^{-1}$ with the white dwarf reaching a peak temperature of ~50,000 K.
3. The motion of the UV absorption lines throughout the orbit is very small, with the best measurements yielding a K_{wd} of 7.6 ± 0.8 km s^{-1}, consistent with a relatively high-mass white dwarf.
4. From the UV lines, the gravitational redshift of the white dwarf is determined to be 47 km s^{-1}, similar to the value determined by van Spaandonk et al. (2010a), implying a white dwarf mass of 0.8 $M_\odot$.
5. The fit to the pronounced, resolved UV lines of Si II indicates a rotation velocity of 40 km s^{-1} for the white dwarf, implying a spin period of 209 s for a radius of 7000 km and an inclination of 11 deg.

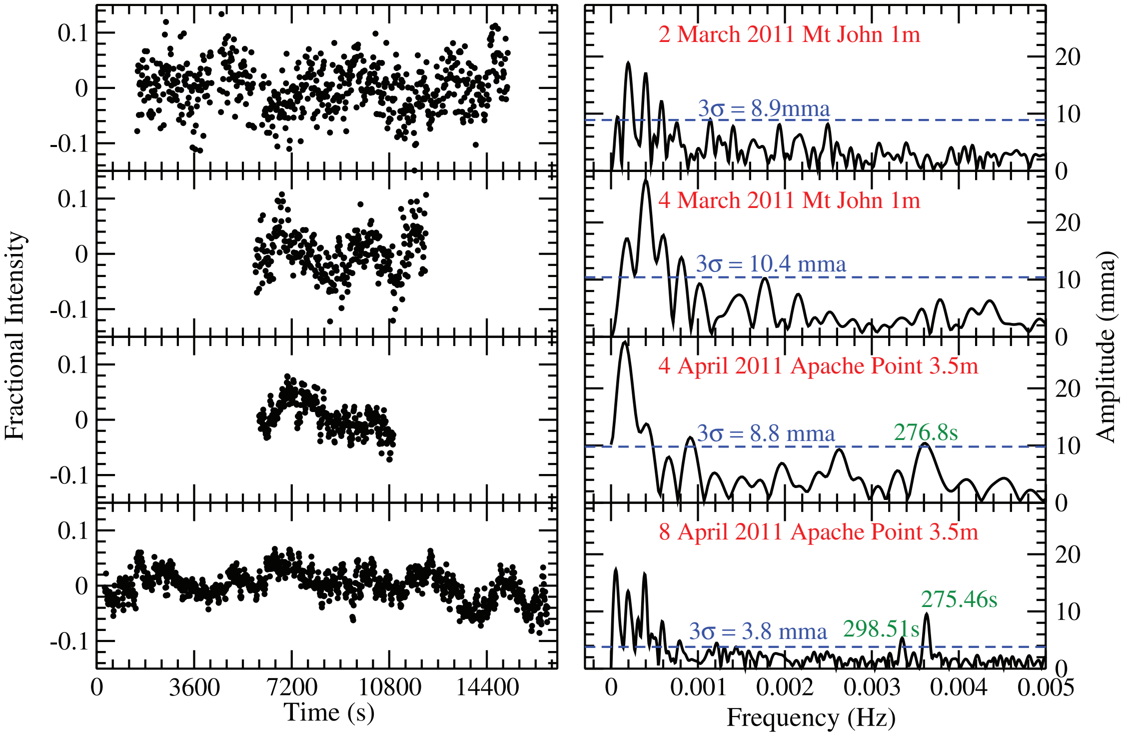

Figure 12. Intensity light curves and DFTs of MJUO and APO optical data from 2011 March–April.

(A color version of this figure is available in the online journal.)

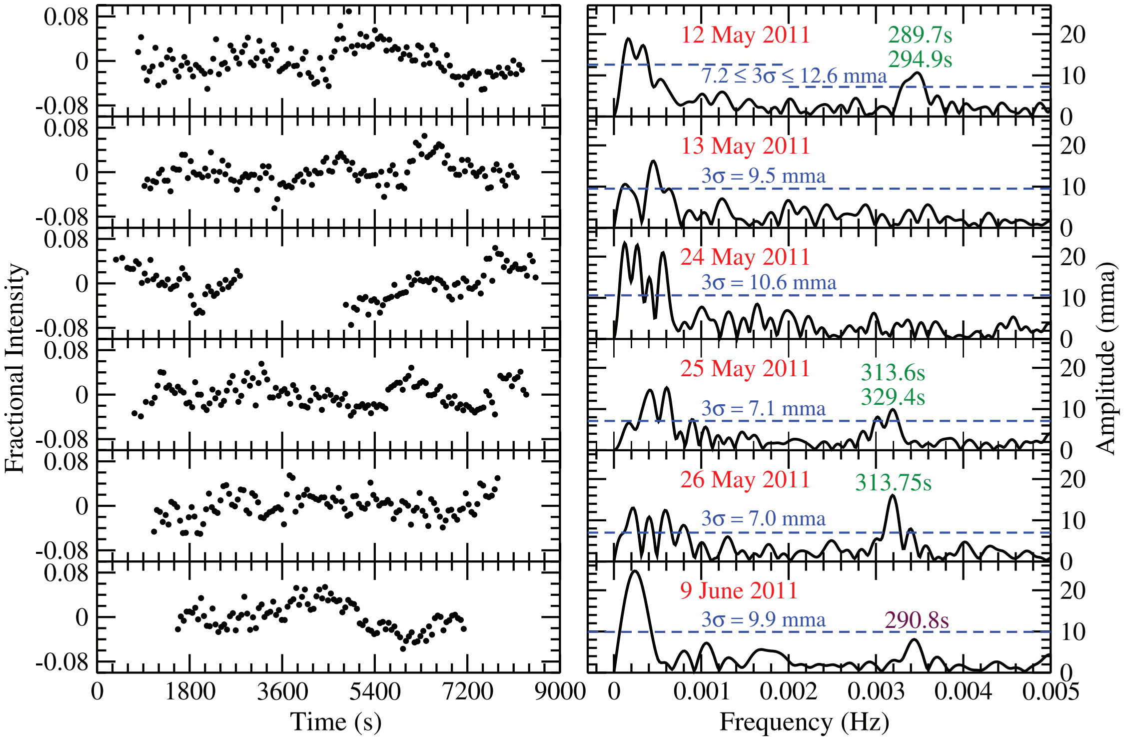

Figure 13. Intensity light curves and DFTs from KPNO data during 2011 May–June.

(A color version of this figure is available in the online journal.)

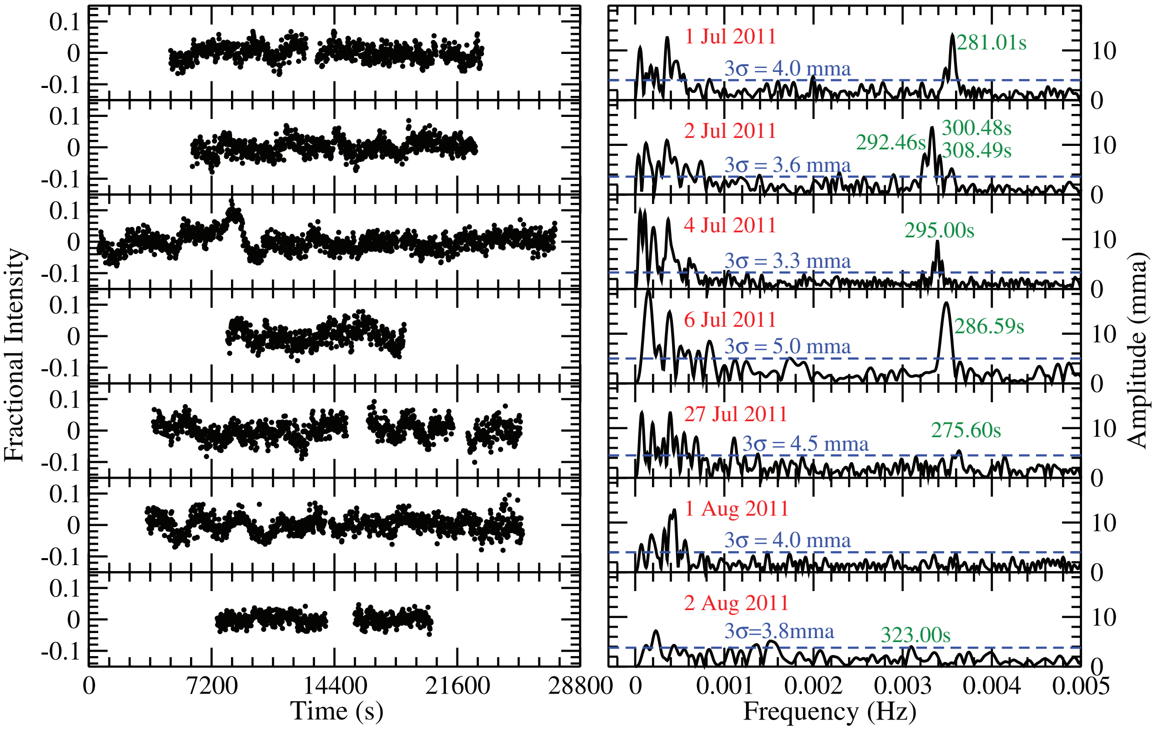

Figure 14. Intensity light curves and DFTs from MJUO data during 2011 July–August.

(A color version of this figure is available in the online journal.)

6. At both three and four years past outburst, the UV data show closely spaced periods near 290 s which appear to be a multiplet. While these periods show increased amplitudes in the UV over the optical (factor of ∼5), consistent with limb-darkening expectations for non-radial pulsations, and double in amplitude from 2010 to 2011, the periods are intermittent and very different from the pulsation spectrum seen at quiescence. It remains to be seen if this is indeed the return of the pulsations.

Our results strengthen past ideas that a large amplitude outburst can heat the white dwarf and result in cooling times of years (Sion 1995; Godon et al. 2006), that the mean mass of

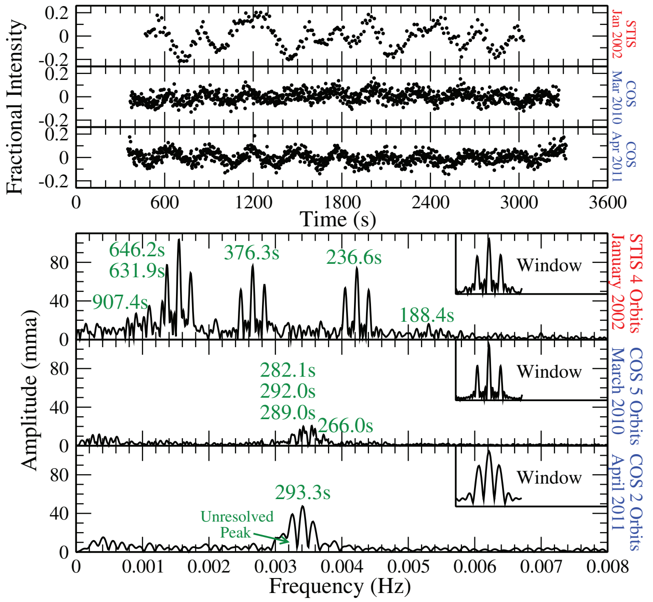

Figure 15. Comparison of intensity light curves and DFTs from 2002 STIS quiescent data to those from COS 2010 and 2011.

(A color version of this figure is available in the online journal.)

the white dwarfs in cataclysmic variables is larger than that for single white dwarfs (Zorotovic et al. 2011), and that they are rotating much faster than their single counterparts, although not near breakup velocity. However, the results on the non-radial pulsations are not as clear. If the period near 290 s is the return of the pulsations, its multiplet structure, which cannot be due to a slow spin of the white dwarf, and its intermittent and changing frequency remain a puzzle. As GW Lib has still not reached its quiescent temperature, further monitoring will still be required to determine how the interior of the white dwarf has reacted to its outburst. The evolution of the pulsation spectrum is unlike that evident in the accreting pulsator SDSS0745+45, which returned to its quiescent pulsation spectrum within 3.3 years (Mukadam et al. 2011b), but then turned off during later observations (A. S. Mukadam, in preparation), or of SDSS0804+51, in which pulsations appeared one year after outburst (Pavlenko 2009; Pavlenko et al. 2011), but were not apparent later during quiescence. It remains unclear if the pulsations in these accreting systems can turn on and off due to small accretion changes as well as from large outbursts which heat the white dwarf dramatically. Long-term monitoring programs on dedicated stars will be required to sort out all the details.

We gratefully acknowledge Elizabeth Waagen, Matthew Templeton, and the observers of the AAVSO for their efforts in monitoring the brightness state of GW Lib that allowed the *HST* observations to proceed, especially Bob Koff, Peter Lake, Mike Linnolt, Hazel McGee, Mike Simonsen, Chris Stockdale, and Rod Stubbings, as well as Howard Bond for providing measurements from SMARTS. We also acknowledge the LCOGT for providing observing time. This work was supported by NASA grants HST-GO1163.01A, HST-GO11639-01A, and HST-GO12231.01A from the Space Telescope Science Institute, which is operated by the Association of Universities for Research in Astronomy, Inc., for NASA, under contract NAS 5-26555, and by the NSF grant AST-1008734. D.J.S. and P.C. acknowledge financial support from the NZ Marsden Fund. E.J.H. acknowledges support by the M. J. Murdock Charitable Trust.

REFERENCES

Araujo-Betancor, S., Gänsicke, B. T., Hagen, H.-J., et al. 2005, A&A, 430, 629
Arras, P., Townsley, D. M., & Bildsten, L. 2006, ApJ, 643, L119
Bullock, E., Szkody, P., Mukadam, A. S., et al. 2011, AJ, 141, 84
Clemens, J. C. 1993, PhD thesis, Univ. Texas
Copperwheat, C. M., Marsh, T. R., Dhillon, V. S., et al. 2009, MNRAS, 393, 157
Gänsicke, B. T., Szkody, P., Howell, S. B., & Sion, E. M. 2005, ApJ, 629, 451
Godon, P., Sion, E. M., Cheng, F., et al. 2006, ApJ, 642, 1018
Gonzalez, L. E., & Maza, J. 1983, IAU Circ., 3854
Howell, S. B., Szkody, P., & Cannizzo, J. K. 1995, ApJ, 439, 337
Hubeny, I., & Lanz, T. 1995, ApJ, 439, 875
Kato, T., Maehara, H., & Monard, B. 2008, PASJ, 60, 23
Kepler, S. O. 1993, Balt. Astron., 2, 515
Kleinman, S. J., Nather, R. E., Winget, D. E., et al. 1998, ApJ, 495, 424
Long, K. S., Froning, C. S., Gänsicke, B., et al. 2003, ApJ, 591, 1172
Long, K. S., Sion, E. M., Huang, M., & Szkody, P. 1994, ApJ, 424, L49
Montgomery, M. H. 2005, ApJ, 633, 1142
Mukadam, A. S., Montgomery, M. H., Winget, D. E., Kepler, S. O., & Clemens, J. C. 2006, ApJ, 640, 956
Mukadam, A. S., Owen, R., Mannery, E., et al. 2011a, PASP, 123, 1423
Mukadam, A. S., Townsley, D. M., Gänsicke, B. T., et al. 2010, ApJ, 714, 1702
Mukadam, A. S., Townsley, D. M., Szkody, P., et al. 2011b, ApJ, 728, L33
Nather, R. E., & Mukadam, A. S. 2004, ApJ, 605, 846
Patterson, J., Kemp, J., Harvey, D. A., et al. 2005, PASP, 117, 1204
Pavlenko, E. 2009, J. Phys.: Conf. Ser., 172, 2071
Pavlenko, E., et al. 2011, arXiv:1111.2339
Piro, A. L., Arras, P., & Bildsten, L. 2005, ApJ, 628, 401
Robinson, E. L., Mailloux, T. M., Zhang, E., et al. 1995, ApJ, 438, 908
Schwieterman, E. W., et al. 2010, J. Southeastern Assoc. Res. Astron., 3, 6
Sion, E. M. 1995, ApJ, 438, 876
Sion, E. M., Cheng, F. H., Szkody, P., et al. 1998, ApJ, 496, 449
Sion, E. M., Huang, M., Szkody, P., & Cheng, F. H. 1995, ApJ, 445, L31
Sion, E. M., Long, K. S., Szkody, P., & Huang, M. 1994, ApJ, 430, L53
Steeghs, D., Howell, S. B., Knigge, C., et al. 2007, ApJ, 667, 442
Szkody, P., Gänsicke, B. T., Howell, S. B., & Sion, E. M. 2002, ApJ, 575, L79
Szkody, P., Mukadam, A., Gänsicke, B. T., et al. 2010, ApJ, 710, 64
Templeton, M., Stubbings, R., Waagen, E. O., et al. 2007, CBET, 922, 1
Thorstensen, J. R. 2003, AJ, 126, 3017
Thorstensen, J. R., Patterson, J., Kemp, J., & Vennes, S. 2002, PASP, 114, 1108
Townsley, D. M., Arras, P., & Bildsten, L. 2004, ApJ, 608, L105
Uthas, H., Patterson, J., Kemp, J., et al. 2012, MNRAS, 420, 379
van Spaandonk, L., Steeghs, D., Marsh, T. R., & Parsons, S. G. 2010a, ApJ, 715, L109
van Spaandonk, L., Steeghs, D., Marsh, T. R., & Torres, M. A. P. 2010b, MNRAS, 401, 1857
van Zyl, L., Warner, B., O'Donohue, D., et al. 2000, Balt. Astron., 9, 231
van Zyl, L., Warner, B., O'Donoghue, D., et al. 2004, MNRAS, 350, 307
Vican, L., Patterson, J., Allen, W., et al. 2011, PASP, 123, 1156
Warner, B., & van Zyl, L. 1998, in IAU Symp. 185, New Eyes to See Inside the Sun and Stars, ed. F.-L. Deubner, J. Christensen-Dalsgaard, & D. Kurtz (Dordrecht: Kluwer), 321
Zorotovic, M., Schreiber, M. K., & Gänsicke, B. T. 2011, A&A, 536, 42